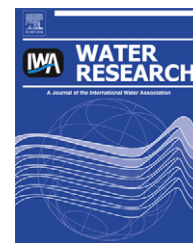


Available at www.sciencedirect.comjournal homepage: www.elsevier.com/locate/watres

Biological Cr(VI) removal coupled with biomass growth, biomass decay, and multiple substrate limitation

E.M. Contreras^{a,b,*}, A.M. Ferro Orozco^a, N.E. Zaritzky^{a,b}

^aCentro de Investigación y Desarrollo en Criotecología de Alimentos (CIDCA), CCT La Plata CONICET, Fac. de Cs. Exactas, UNLP. 47 y 116, B1900AJJ La Plata, Argentina

^bFac. de Ingeniería, UNLP. 47 y 1, B1900AJJ La Plata, Argentina

ARTICLE INFO

Article history:

Received 26 October 2010

Received in revised form

2 February 2011

Accepted 8 March 2011

Available online 16 March 2011

Keywords:

Cr(VI) reduction

Chromium toxicity

Kinetic parameter

Activated sludge

Nitrogen to carbon ratio

Mathematical modeling

ABSTRACT

In this work, a mathematical model for the biological reduction of Cr(VI), carbon and nitrogen sources consumption, and biomass growth under fully aerobic conditions was developed. The model comprises three types of aerobic heterotrophic cells (non-growing cells, growing cells with chromate reductase activity, and growing cells that have lost the chromate reductase activity), and five soluble compounds (organic substrate, ammonia nitrogen, non-metabolizable soluble products, dissolved oxygen, and hexavalent chromium). Two processes are considered responsible for the reduction of Cr(VI). The first one is the reduction of Cr(VI) coupled with growth, the second process is coupled with the endogenous decay of the biomass. The model was calibrated using the results obtained in batch cultures in the absence of carbon and nitrogen sources, using different initial Cr(VI) concentrations (0–100 mgCr L⁻¹), two carbon sources (cheese whey and lactose), and different initial nitrogen to carbon ratio (0–50 mgN gCOD⁻¹). The calibrated model was used to calculate steady-state values of TSS, soluble COD, TAN and Cr(VI) in continuous systems, obtaining a good agreement with the experimental data. The model also accurately predicted the transient concentration of Cr(VI) as a function of time in response to step changes of the inlet Cr(VI) concentration in continuous systems.

© 2011 Elsevier Ltd. All rights reserved.

1. Introduction

Biotransformation of metals is a promising technique to convert more toxic heavy metals into less toxic forms, and therefore, can be potentially useful for bioremediation of industrial wastewaters. A good example of biotransformation is the case of chromium.

The extensive use of chromium in several industries such as petroleum refining, metal finishing, leather tanning, iron and steel industries, inorganic chemical production, textile manufacturing and pulp production have largely contributed to its wide spread in the environment (Katz and Salem, 1994;

Guertin et al., 2005). Although chromium has several oxidation states, chromium compounds mainly occur as Cr(III) or Cr(VI). The former is the most stable under reduced conditions, it is relatively immobile because it has a strong affinity for negative charged ions and colloids in soils, and gives sparingly soluble compounds such as Cr(OH)₃ that dominate at pH values from 4 to 8. Conversely, Cr(VI) is more soluble, mobile, and bio-available than Cr(III). Cr(VI) occurs in the form of oxoanions under most environmental conditions. Equilibria of hexavalent chromium compounds are pH and concentration dependent. Chromate ion (CrO₄²⁻) represents more than 98% of the total Cr(VI) species for pH higher than 8. Chromate

* Corresponding author. Centro de Investigación y Desarrollo en Criotecología de Alimentos (CIDCA), CCT La Plata CONICET, Fac. de Cs. Exactas, UNLP. 47 y 116, B1900AJJ La Plata, Argentina. Tel./fax: +54 221 4254853.

E-mail address: edgardo.contreras@ing.unlp.edu.ar (E.M. Contreras).

0043-1354/\$ – see front matter © 2011 Elsevier Ltd. All rights reserved.

doi:10.1016/j.watres.2011.03.011

Nomenclature*Model compounds*Cr (mgCr L⁻¹) soluble hexavalent chromium concentrationS (mgCOD L⁻¹) organic substrate concentrationP (mgCOD L⁻¹) soluble products concentration released during the biomass decayNH (mgN L⁻¹) total ammonia nitrogen (TAN) concentrationX_{NG} (mgCOD L⁻¹) non-growing biomass concentrationX_{GA} (mgCOD L⁻¹) growing active (with chromate reductase activity) biomass concentrationX_{GNA} (mgCOD L⁻¹) growing non-active (without chromate reductase activity) biomass concentration*Stoichiometric coefficients*Y (mgCOD mgCOD⁻¹) true biomass yieldi_{N,BM} (mgN mgCOD⁻¹) nitrogen content of the biomassi_{N,P} (mgN mgCOD⁻¹) nitrogen content of the products released during the endogenous decayf_P (mgCOD mgCOD⁻¹) fraction of the endogenous biomass converted into soluble inert productsR_C (mgCr mgCOD⁻¹) Cr(VI) removed per unit mass of X_{GA} converted into X_{GNA}i_{SS} (mgTSS mgCOD⁻¹) conversion factor from biomass COD to TSS units*Kinetic coefficients*k_A (h⁻¹) first order lag phase constantμ_{m0} (h⁻¹) maximum specific growth rate in the absence of Cr(VI)μ_{m∞} (h⁻¹) maximum specific growth rate at infinite Cr(VI)q_{Sm0} (mgCOD mgCOD⁻¹ h⁻¹) maximum specific substrate consumption rate in the absence of Cr(VI)q_{Sm∞} (mgCOD mgCOD⁻¹ h⁻¹) maximum specific substrate consumption rate at infinite Cr(VI) concentrationK (L mgCr⁻¹) inhibition constant due to Cr(VI) toxicityK_S (mgCOD L⁻¹) half-saturation coefficient for SK_{NH} (mgN/L) half-saturation coefficient for NHb (h⁻¹) specific endogenous decay rateq_{CrGm} (mgCr mgCOD⁻¹ h⁻¹) maximum specific Cr(VI) consumption rate associated to the growth phaseq_{CrDm} (mgCr mgCOD⁻¹ h⁻¹) maximum specific Cr(VI) consumption rate associated to the decay phase

monoacid (HCrO₄⁻), and dichromate (Cr₂O₇²⁻) ions are the main species when pH is lower than 5. In addition, as the total Cr(VI) concentration increases, the fraction of HCrO₄⁻ decreases due to the formation of dichromate. In all cases, the fraction of chromic acid (H₂CrO₄) is negligible. Within the normal pH range of most biological wastewater treatment systems (pH about 5–9) and for Cr(VI) concentrations usually found in wastewaters (usually less than 2 mM), Cr₂O₇²⁻ ion account for less than 3% of the total Cr(VI); thus, HCrO₄⁻ and CrO₄²⁻ are the dominant species (Contreras et al., in press).

The reduction of Cr(VI) to Cr(III) is of great environmental importance, because Cr(III) is less hazardous. Chromium is an essential micro-nutrient in the diet of animals and humans, as it is indispensable for the normal sugar, lipid and protein metabolism of mammals (USEPA, 1998a). Conversely, Cr(VI) is highly toxic to all forms of living organisms, mutagenic in bacteria, mutagenic and carcinogenic in humans and animals (USEPA, 1998b). For these reasons, reducing Cr(VI) to Cr(III) is beneficial in eliminating the toxicity of Cr(VI) from the environment.

For many years, conventional Cr(VI) removal was achieved by chemical reduction, ion exchange or adsorption. Recently, researchers have focused attention on bioremediation of hexavalent chromium. In contrast to the conventional methods, bioremediation is cost-effective (Li et al., 2007). Trivalent and hexavalent forms of chromium can interconvert; within normal conditions, the reduction of Cr(VI) to Cr(III) due to the presence of organic compounds is favored. For example, the change of free energy at pH 7.0 and 25 °C corresponding to the reaction between acetic acid (electron donor) and chromate ion (electron acceptor) is about -83.3 kJ per mole of electrons transferred. Thus, from a thermodynamic point of view, Cr(VI) is capable of oxidizing acetic acid and also most of the organic compounds commonly found in wastewaters (Contreras et al., in press). However, the

reduction of Cr(VI) to Cr(III) by organic compounds is frequently slow; thus, in the absence of a catalyst, such as the activated sludge biomass, redox systems are far from equilibrium (Stumm and Morgan, 1996). Therefore, the presence of cells that act as catalyst, and a suitable electron donor are necessary to achieve the reduction of Cr(VI).

The ability of Cr(VI) reduction has been found in many bacterial genera including *Pseudomonas*, *Micrococcus*, *Bacillus*, *Achromobacter*, *Microbacterium*, *Arthrobacter*, and *Corynebacterium* (McLean et al., 2000; Pattanapitpaisal et al., 2001; McLean and Beveridge, 2001; Megharaj et al., 2003). The mechanisms through which bacterial strains reduce Cr(VI) to Cr(III) are variable and species dependent (McLean et al., 2000). Anaerobic bacteria may use chromate as a terminal-electron acceptor or reduce chromate in periplasmic space by hydrogenase or cytochrome c3 (Michel et al., 2001; Puzon et al., 2002). In aerobic bacteria, Cr(VI) reduction may be carried out by cellular reducing agents (the primary reductant is glutathione) and NADH-dependent chromate reductase (Shen and Wang, 1994; Garbisu et al., 1998). The mechanisms for Cr(VI) reduction might be a secondary utilization or cometabolism as suggested for *Shewanella onoidensis* MR-1 (Middleton et al., 2003).

Although there are many studies concerning the removal of Cr(VI) by pure cultures of different microorganisms, its applicability to field removal processes is limited. The main disadvantage of using pure cultures to remove chromium compounds is related to the use of sterile conditions to prevent external microbial contamination, increasing the treatment costs. If sterile conditions are not employed (due to economic reasons, for example), indigenous bacteria may overcome the added Cr(VI)-reducing microorganisms. Besides, most countries have severe restrictions concerning the introduction of new species. For these reasons, results obtained in the study of Cr(VI) removal by mixed cultures,

such as activated sludge, are more relevant to optimize design and operation of actual biological Cr(VI) reduction systems.

Many factors affect the reduction of Cr(VI) by activated sludge. In previous works it was demonstrated that the presence of suitable carbon and nitrogen sources are necessary to enhance the Cr(VI) reduction capacity of activated sludge (Ferro Orozco et al., 2007, 2010a). Several studies (Shen and Wang, 1994; Wang and Shen, 1995, 1997) demonstrated that the rate and extent of Cr(VI) reduction in batch cultures depend on the initial biomass concentration, regardless of the subsequent growth. Recently, Ferro Orozco et al. (2010a) demonstrated that the net biological Cr(VI) removal is the consequence of two processes: a fast Cr(VI) removal process, associated to the biomass growth, and a slow removal process that is independent of the presence of both the carbonaceous substrate and the nitrogen source. While the former process is important when there is no limitation in carbon or nitrogen sources (within the exponential growth phase in batch systems, for example), the latter may be significant in continuous cultures in which substrate concentrations are normally low (Ferro Orozco et al., 2010a).

The utilization of biological processes for the treatment of wastewaters containing toxic compounds, such as Cr(VI), emphasizes the practical requirement for developing adequate mathematical models to be used for the design and operation of these processes. The knowledge of microbial substrate utilization kinetics and the effect of toxic compounds on the growth rate are both important for the accurate prediction of the quality of the treatment process effluent. Accurate models and kinetic parameters also help engineers to optimize operational conditions in order to meet discharge requirements minimizing the operational costs.

In this work, a mathematical model that describes the biological removal of Cr(VI) coupled with biomass growth, biomass decay, and multiple substrate limitation was developed. The model takes into account the effect of the initial Cr(VI) and substrates (carbon and nitrogen sources) concentrations, and Cr(VI) toxicity on the observed growth rate of activated sludge and on Cr(VI) removal. The model was calibrated using batch experiments under different conditions, and it was validated by comparing model results with those obtained in continuous systems.

2. Mathematical model

2.1. General description

Three types of aerobic heterotrophic cells were considered in the model: non-growing cells (X_{NG}), growing cells with chromate reductase activity (X_{GA}), and growing cells that have lost the chromate reductase activity (X_{GNA}). Non-growing cells (X_{NG}) are converted to growing cells with chromate reductase activity (X_{GA}) following a first order kinetics; this process was introduced to simulate the lag phase observed in batch cultures (Ferro Orozco et al., 2010b). In addition, due to toxic effects of Cr(VI), X_{GA} cells lose its chromate reductase activity to produce X_{GNA} (Yamamoto et al., 1993; Wang and Shen, 1997; Ferro Orozco et al., 2008). Organic substrate (S) and ammonia nitrogen (NH) can limit the growth rate of X_{GA} and X_{GNA} ; for

this reason, Monod saturation terms corresponding to each substrate were included. Under endogenous decay, the three types of cells release non-metabolizable soluble products (P), and ammonia nitrogen (NH). Growth of X_{GA} produces new X_{GA} cells, however, during the growth of X_{GNA} new cells with chromate reductase activity (X_{GA}) are formed. In addition, to reduce model complexity, growth kinetics corresponding to X_{GA} and X_{GNA} were assumed identical.

Two processes are considered responsible for the reduction of Cr(VI) to Cr(III) (Ferro Orozco et al., 2010a). The first one is the reduction of Cr(VI) coupled with the growth of X_{GA} ; during this process some electrons of the organic substrate are transferred to Cr(VI). Although this process is fast, it depends on the availability of S and NH. Because both S and NH can limit the growth of X_{GA} , if one or more of those substrates are absent then this process stops. The second Cr(VI) reduction process is coupled with the endogenous decay of the biomass; in this case, the source of electrons to reduce Cr(VI) is the biomass itself. This process is slower than the first one but not depends on the availability of substrates (Ferro Orozco et al., 2010a).

2.2. Definitions of model compounds

The following compounds are used in the model:

S (mgCOD L⁻¹) = organic substrate concentration, carbon and energy source for biomass growth.

P (mgCOD L⁻¹) = soluble products concentration, released during the biomass decay.

NH (mgN L⁻¹) = total ammonia nitrogen (TAN) concentration, nitrogen source for biomass growth.

X_{NG} (mgCOD L⁻¹) = non-growing biomass concentration (biomass in Lag phase).

X_{GA} (mgCOD L⁻¹) = growing active (with chromate reductase activity) biomass concentration.

X_{GNA} (mgCOD L⁻¹) = growing non-active (without chromate reductase activity) biomass concentration.

Cr (mgCr L⁻¹) = soluble hexavalent chromium concentration.

2.3. Stoichiometry and kinetics

The stoichiometric matrix $\nu_{j,i}$ of the model is shown in Table 1; all empty elements of $\nu_{j,i}$ indicate zero values. The model has six stoichiometric coefficients:

Y (mgCOD mgCOD⁻¹) = true biomass yield

$i_{N,BM}$ (mgN mgCOD⁻¹) = nitrogen content of the biomass

$i_{N,P}$ (mgN mgCOD⁻¹) = nitrogen content of the products released during the endogenous decay

f_P (mgCOD mgCOD⁻¹) = fraction of the endogenous biomass converted into soluble inert products

R_C (mgCr mgCOD⁻¹) = Cr(VI) removed per unit mass of X_{GA} converted into X_{GNA}

i_{SS} (mgTSS mgCOD⁻¹): conversion factor from biomass COD to TSS units

A first order kinetics with a constant k_A was assumed for the conversion of non-growing cells (X_{NG}) to growing cells

Table 1 – Stoichiometric matrix ($\nu_{j,i}$) of the proposed model and process rate expressions (ρ_j).

Process (j)	Compound (i)									Rate (ρ_j)
	1 X_{NG}	2 X_{GA}	3 X_{GNA}	4 S	5 NH	6 DO	7 P	9 Cr		
1 Activation of X_{NG} to X_{GA}	-1	1								$k_A X_{NG}$
2 Growth of X_{GA}		1		$\frac{1}{Y}$	$-i_{N,BM}$	$-\left(\frac{1-Y}{Y}\right)$				μX_{GA}
3 Growth of X_{GNA}		1		$\frac{1}{Y}$	$-i_{N,BM}$	$-\left(\frac{1-Y}{Y}\right)$				μX_{GNA}
4 Decay of X_{NG}	-1				$(i_{N,BM}-i_{N,P})$	$-(1-f_P)$	f_P			$b X_{NG}$
5 Decay of X_{GA}		-1			$(i_{N,BM}-i_{N,P})$	$-(1-f_P)$	f_P			$b X_{GA}$
6 Decay of X_{GNA}					$(i_{N,BM}-i_{N,P})$	$-(1-f_P)$	f_P			$b X_{GNA}$
7 Cr reduction by growth of X_{GA}		$\frac{1}{R_C}$	$\frac{1}{R_C}$					-1		$q_{CrG} X_{GA}$
8 Cr reduction by decay of X_{NG}								-1		$q_{CrD} X_{NG}$
9 Cr reduction by decay of X_{GA}								-1		$q_{CrD} X_{GA}$
Observed conversion rates	$r_i = \sum_j \nu_{j,i} \rho_j$									

where μ , q_S , q_{CrG} , q_{CrD} , and Y are defined by Eqs. (1)–(5), respectively.

with chromate reductase activity (X_{GA}) to simulate the lag phase (Ferro Orozco et al., 2010b). In addition, the following kinetic expressions corresponding to the specific growth rate (μ), specific substrate consumption rate (q_S), specific Cr(VI) consumption rate associated to growth phase (q_{CrG}) and to endogenous decay phase (q_{CrD}) were proposed:

$$\mu = \left[\frac{\mu_{m0} + \mu_{m\infty} KCr}{1 + KCr} \right] \left(\frac{S}{K_S + S} \right) \left(\frac{NH}{K_{NH} + NH} \right) \tag{1}$$

$$q_S = \left[\frac{q_{Sm0} + q_{Sm\infty} KCr}{1 + KCr} \right] \left(\frac{S}{K_S + S} \right) \left(\frac{NH}{K_{NH} + NH} \right) \tag{2}$$

$$q_{CrG} = q_{CrGm} \left(\frac{KCr}{1 + KCr} \right) \left(\frac{S}{K_S + S} \right) \left(\frac{NH}{K_{NH} + NH} \right) \tag{3}$$

$$q_{CrD} = q_{CrDm} \left(\frac{KCr}{1 + KCr} \right) \tag{4}$$

where:

μ_{m0} (h^{-1}) = maximum specific growth rate in the absence of Cr (VI)

$\mu_{m\infty}$ (h^{-1}) = maximum specific growth rate at infinite Cr(VI) concentration

q_{Sm0} ($mgCOD\ mgCOD^{-1}\ h^{-1}$) = maximum specific substrate consumption rate in the absence of Cr(VI)

$q_{Sm\infty}$ ($mgCOD\ mgCOD^{-1}\ h^{-1}$) = maximum specific substrate consumption rate at infinite Cr(VI) concentration

K ($L\ mgCr^{-1}$) = inhibition constant due to Cr(VI) toxicity

K_S ($mgCOD\ L^{-1}$) = half-saturation coefficient for S

K_{NH} ($mgN\ L^{-1}$) = half-saturation coefficient for NH

b (h^{-1}) = specific endogenous decay rate

q_{CrGm} ($mgCr\ mgCOD^{-1}\ h^{-1}$) = maximum specific Cr(VI) consumption rate associated to growth

q_{CrDm} ($mgCr\ mgCOD^{-1}\ h^{-1}$) = maximum specific Cr(VI) consumption rate associated to decay

Eqs. (1) and (2) take into account the toxic effect of Cr(VI) on the specific growth rate (μ) and specific substrate consumption (q_S) of activated sludge. The removal of Cr(VI) associated with the growth and the endogenous decay of activated sludge were represented by Eqs. (3) and (4), respectively. Because

both carbon (S) and nitrogen sources (NH) can limit the growth process, Monod-type saturation terms were included.

The true biomass growth yield (Y) can be calculated by combining Eqs. (1) and (2) as follows:

$$Y = \frac{\mu}{q_S} \tag{5}$$

From model outputs, soluble COD (COD_S), total suspended solids (TSS), and oxygen uptake rate (OUR) can be computed as follows:

$$COD_S = S + P \tag{6}$$

$$TSS = i_{SS}(X_{NG} + X_{GA} + X_{GNA}) \tag{7}$$

$$OUR = \left(\frac{1-Y}{Y} \right) \mu (X_{GA} + X_{GNA}) + (1-f_P) b (X_{NG} + X_{GA} + X_{GNA}) \tag{8}$$

It must be pointed out that the present model was developed for fully aerobic conditions. Aeration conditions were assumed high enough as to maintain the dissolved oxygen (DO) close to the saturation level. However, if this is not the case, Eqs. (1)–(3) can be modified to include Monod saturation terms corresponding to DO. Although the model allowed predicting the OUR (Eq. 8), the effect of the DO concentration on the kinetics is out of the scope of the present work.

3. Materials and methods

3.1. Biological and chemical materials

All reagents used in the present work were commercial products of reagent grade from Anedra (San Fernando, Argentina). Activated sludge used in all the experiments were harvested from a continuous aerobic laboratory-scale (4.5 L) activated sludge reactor with partial biomass recycle. Aeration was provided by an air pump; air was pumped near the bottom of the reactor and it was enough to maintain the dissolved oxygen concentration above $4\ mgO_2\ L^{-1}$. The reactor was fed with a synthetic wastewater with the following composition: dehydrated cheese whey (Food S.A. Villa Maipú, Argentina)

1.5 g, $(\text{NH}_4)_2\text{SO}_4$ 0.90 g, and NaHCO_3 1.03 g dissolved in 1 L of tap water. Soluble chemical oxygen demand (COD_s) of the synthetic wastewater was 1500 mg L^{-1} . The hydraulic retention time was 2 d; the sludge age was maintained at 45 d by daily wasting of mixed liquor directly from the reactor. During the experiments the temperature of the reactor was $20 \pm 2 \text{ }^\circ\text{C}$. Under steady-state conditions dissolved oxygen concentration (DO) was above 4 mg L^{-1} , pH was 7.9 ± 0.5 , COD_s of the effluent ranged between 30 and 160 mg L^{-1} , and total suspended solid (TSS) concentration ranged from 3700 to $5400 \text{ mg TSS L}^{-1}$.

3.2. Cr(VI) removal by activated sludge in different systems

3.2.1. Cr(VI) removal in the absence of substrates

The removal of Cr(VI) under endogenous decay conditions of activated sludge were studied in 250 mL aerated vessels at constant temperature ($20 \pm 2 \text{ }^\circ\text{C}$) and initial pH = 7.0 ± 0.1 . Small air pumps were employed to aerate and to agitate the vessels. Air was pumped near the bottom of each vessel via a flexible hose; aeration was enough to maintain the dissolved oxygen concentration above $5 \text{ mg O}_2 \text{ L}^{-1}$. Activated sludge samples were obtained from the reactor described previously (Section 3.1). The samples were washed three times with phosphate buffer (KH_2PO_4 2 g L^{-1} , K_2HPO_4 0.5 g L^{-1} , pH = 7) before performing the assays in order to remove all remnant of substrates. Activated sludge washed samples were re-suspended in phosphate buffer to obtain an initial biomass concentration of $3800 \pm 200 \text{ mg TSS L}^{-1}$. A Cr(VI) stock solution ($10 \text{ g Cr(VI) L}^{-1}$) was prepared using analytical grade $\text{K}_2\text{Cr}_2\text{O}_7$; an appropriate volume of this solution was added to obtain 10–100 mg Cr(VI) L^{-1} . At predetermined time intervals, samples were withdrawn from the vessels to determine biomass (X), soluble COD (COD_s), total ammonia nitrogen (TAN), and Cr(VI) concentrations.

3.2.2. Effect of Cr(VI) on activated sludge growth and Cr(VI) removal

These experiments were performed in 250 mL aerated vessels at room temperature ($20 \pm 2 \text{ }^\circ\text{C}$) and initial pH = 7.0 ± 0.1 . Activated sludge samples were washed before performing the assays. In these experiments the initial biomass concentration was $700 \pm 50 \text{ mg TSS L}^{-1}$. The culture medium composition was the following: dehydrated cheese whey (carbon and energy source) 5 g COD L^{-1} , ammonium sulfate (nitrogen source) 212 mg N L^{-1} , and micro-nutrient solutions M1 and M2 (1 mL L^{-1}). The composition of M1 was (expressed as g 100 mL^{-1}): $\text{FeSO}_4 \cdot 7\text{H}_2\text{O}$ 1.5, $\text{ZnSO}_4 \cdot 7\text{H}_2\text{O}$ 0.5, $\text{MnSO}_4 \cdot \text{H}_2\text{O}$ 0.3, $\text{CuSO}_4 \cdot 5\text{H}_2\text{O}$ 0.075, $\text{CoCl}_2 \cdot 6\text{H}_2\text{O}$ 0.015, and citric acid 0.6. M2 solution contained the following salts (g 100 mL^{-1}): $(\text{NH}_4)_6\text{Mo}_7\text{O}_{24} \cdot 4\text{H}_2\text{O}$ 0.05, BO_3H_3 0.01, KI 0.01. Tested Cr(VI) concentrations were 0, 10, 25, 50, and 100 mg L^{-1} . At predetermined time intervals samples were taken to determine biomass (X), soluble COD (COD_s), and Cr(VI) concentrations, and oxygen uptake rate (OUR).

3.2.3. Effect of the initial nitrogen to carbon ratio (N_0/S_0) on activated sludge growth and Cr(VI) removal

Cr(VI) removal batch assays, similar to those described in the previous section, were performed. Because the cheese whey

provides not only organic matter but also organic nitrogen, cheese whey was replaced by lactose in order to control the initial nitrogen to carbon ratio (N_0/S_0). Therefore, in these experiments the culture medium composition was the following: lactose (carbon and energy source) 5.6 g COD L^{-1} , ammonium sulfate (nitrogen source) 0 to 250 mg N L^{-1} , and micro-nutrient solutions M1 and M2 (1 mL L^{-1}). At predetermined time intervals, biomass (X), soluble COD (COD_s), total ammonia nitrogen (TAN), and Cr(VI) concentrations were measured.

3.2.4. Cr(VI) removal in continuous systems

The removal of Cr(VI) in continuous systems was also studied. These experiments were performed in the activated sludge reactors described in Section 2.1. Two sludge ages (θ_c) were tested 20 and 45 d; sludge age was maintained at the desired value by daily wasting of mixed liquor directly from the reactor. In both cases the hydraulic retention time was 2 d. The synthetic wastewater described in Section 2.1 was used to feed the reactors; an appropriate volume of a Cr(VI) stock solution ($10 \text{ g Cr(VI) L}^{-1}$) was added to the synthetic wastewater to obtain the desired inlet Cr(VI) concentration. For $\theta_c = 20$ d, the tested inlet Cr(VI) concentrations were 0, 10, 25, and 50 mg Cr L^{-1} ; for $\theta_c = 45$ d, 0 and 10 mg Cr L^{-1} were tested. Reactors were considered to run under steady-state conditions after operating for one sludge age, at least. Then, samples were withdrawn from the reactor to determine biomass (X), soluble COD (COD_s), total ammonia nitrogen (TAN), and Cr(VI) concentrations.

3.3. Analytical techniques

Total suspended solids (TSS, mg L^{-1}) were used to measure the biomass concentration (X). Known sample volumes (8 mL in this work) were poured into pre-weighted centrifuge tubes, centrifuged and washed twice with distilled water, and placed at $105 \text{ }^\circ\text{C}$ for 24 h; TSS of each sample was calculated as the difference between final weight (dry sample + tube) and initial weight (tube alone) divided by the sample volume. It must be pointed out that TSS is a lumped parameter that included the three types of aerobic heterotrophic cells: non-growing cells (X_{NG}), growing cells with chromate reductase activity (X_{GA}), and growing cells that have lost the chromate reductase activity (X_{GNA}). In all batch growth experiments duplicate biomass measurements were performed to reduce experimental errors; mean and maximum errors for TSS were 4 and 13%, respectively.

Soluble chemical oxygen demand (CODs) was determined as follows: 3 mL of culture samples were centrifuged for 5 min at 13 000 rpm (Eppendorf 5415C); then, the supernatant was filtered through $0.45 \text{ } \mu\text{m}$ cellulosic membranes (Osmonics Inc.). Soluble COD of the filtrate was determined using commercial reagents (Hach Company, Loveland, CO).

Total ammonia nitrogen (TAN) concentration of the filtrate was measured by the Nessler colorimetric method using commercial reagents (Hach Company, Loveland, CO).

Cr(VI) of the filtrate was determined colorimetrically using a spectrophotometer (Hach DR 2000) at 540 nm by reaction with 1,5-diphenylcarbazide in acid solution (APHA, 2005).

Oxygen uptake rate (OUR, $\text{mgO}_2 \text{ L}^{-1}$) measurements were performed using a closed respirometer consisted in a 30 mL glass vessel maintained at 20 ± 0.5 °C by means of a water bath. The vessel was filled with the tested sample, air was supplied until oxygen saturation level was reached; then, the vessel was sealed with the insertion of a polarographic oxygen probe (YSI model 5739). The sample was continuously stirred with a magnetic stirring and the decay of the dissolved oxygen (DO) concentration as a function of time was recorded. Data were acquired by a personal computer interfaced to the DO monitor (YSI model 58). OUR was calculated as the slope of the straight line obtained by plotting the DO concentration as a function of time.

All the results reported in the present work are average values of two experiments, at least.

3.4. Estimation of the model coefficients and dynamic simulations

The estimation of the coefficients of the mathematical model proposed in this paper and the dynamic simulations were performed using the software package Gepasi 3 (Mendes, 1993). Gepasi integrates the systems of differential equations with the routine LSODA (Livermore Solver of Ordinary Differential Equations). LSODA algorithm measures the stiffness of the equations and switches the integration method dynamically according to this measure. For non-stiff regions, the Adams integration method with variable step size and variable order up to 12th order is used; for stiff regions the Gear (or BDF) method with variable step size and variable order up to 5th order is used. Among the optimization methods available in Gepasi 3, the Multistart Optimization algorithm (with Levenberg–Marquardt local optimization) was selected. Multistart is a hybrid stochastic-deterministic optimization method. Rather than run a simple local optimization (e.g. gradient descent methods), Multistart runs several of them, each time starting from a different initial guess. The first start takes for initial guess the parameter values entered by the user. The initial guesses for the subsequent starts are generated randomly within the boundaries for the adjustable parameters. The local optimizer used is the Levenberg–Marquardt method as this has proved the most efficient gradient optimizer used in Gepasi 3. In order to reduce fitting errors of the adjustable coefficients, initial concentrations were adjusted within $\pm 5\%$ of their measured values. This procedure takes into account the degree of uncertainty in the initial conditions due to analytical errors (Mendes and Kell, 1998). For more details see the [supplementary data](#).

4. Results and discussion

4.1. Cr(VI) removal in the absence of substrates

In order to study the effect of Cr(VI) on the endogenous decay of activated sludge, Cr(VI) removal experiments in the absence of substrates were performed. Fig. 1 shows that no trend can be observed with regard to the biomass decay, ammonia release, and soluble COD production as a function of the initial Cr(VI) concentration. These results indicate that Cr(VI) exerted

a negligible effect on the decay rate of activated sludge; therefore, for modeling purposes a unique value corresponding to the endogenous decay rate constant (b) was assumed. This approach was also adopted by other authors (Elangovan and Philip, 2009).

The proposed model was fitted to the data shown in Fig. 1 to obtain the following coefficients: b , $i_{N,P}$, f_P , and q_{CrDm} (Table 2). Obtained coefficients are within the range reported by other authors. For example, the specific endogenous decay rate (b) obtained in the present work was $(3.3 \pm 0.4) \times 10^{-3} \text{ h}^{-1}$. Elangovan and Philip (2009) reported a value of $b = 0.002 \text{ h}^{-1}$ corresponding to an activated sludge removing Cr(VI) in aerobic batch systems. The default value for the aerobic endogenous respiration rate recommended in the Activated Sludge Model #3 ranged between 0.004 and 0.008 h^{-1} (Gujer et al., 1999). The value corresponding to the specific Cr(VI) consumption rate in the absence of substrates obtained in this work, $q_{CrDm} = (2.2 \pm 1.0) \times 10^{-5} \text{ mgCr mgCOD}^{-1} \text{ h}^{-1}$, is close to the value reported in a previous paper ($q_{CrDm} = 2.3 \times 10^{-5} \text{ mgCr mgCOD}^{-1} \text{ h}^{-1}$) (Ferro Orozco et al., 2010a).

4.2. Effect of Cr(VI) on activated sludge growth and Cr(VI) removal

Fig. 2 shows the time course of biomass (X), soluble COD, oxygen uptake rate (OUR), and Cr(VI) for different initial Cr(VI) concentrations. In all cases, the increase in Cr(VI) concentration produced a longer lag phase; this effect was also reported by other authors (Gikas and Romanos, 2006; Li et al., 2007; Elangovan and Philip, 2009; Gikas et al., 2009; Sengor et al., 2009). After the lag phase, biomass and OUR increased, and soluble COD decreased as a function of time. In all cases, when the soluble COD was depleted, biomass entered to endogenous decay phase and OUR dropped to endogenous levels.

Using the values of b , $i_{N,P}$, f_P , and q_{CrDm} obtained in the previous section (Table 2), the proposed model was fitted to the data shown in Fig. 2 to obtain the following coefficients: μ_{m0} , $\mu_{m\infty}$, q_{Sm0} , $q_{Sm\infty}$, and K (Table 2). Fig. 2 shows that the proposed model predicts satisfactorily the values of soluble COD, X , OUR, and Cr(VI) as a function of time for all the tested conditions.

Although the effect of Cr(VI) on the lag phase was not included explicitly in the proposed model, it was predicted quite well. Taking into account that Cr(VI) exerted a negligible effect on the decay rate of activated sludge (Fig. 1a), this phenomenon can be attributed to the toxic effect of Cr(VI) on μ_m . For this reason, the term between brackets in Eq. (2) was included to represent the inhibition of μ_m as a function of Cr(VI). Because it was assumed that the first order constant (k_A) for the conversion of X_{NG} to X_{GA} was not dependent on the Cr(VI) concentration, the increase of the lag phase was only due to the inhibition of μ_m by Cr(VI). A different approach was used by Gikas et al. (2009) and Sengor et al. (2009) concerning the effect of metals on the lag phase. In the model developed by those authors, the transformation of resting cells to actively growing cells was represented by the metabolic potential function. This function starts at zero value and rises to unity through a convolution of the history of S . Those authors proposed that the lag time is a function of the local metal concentration (Sengor et al., 2009). Although the model of

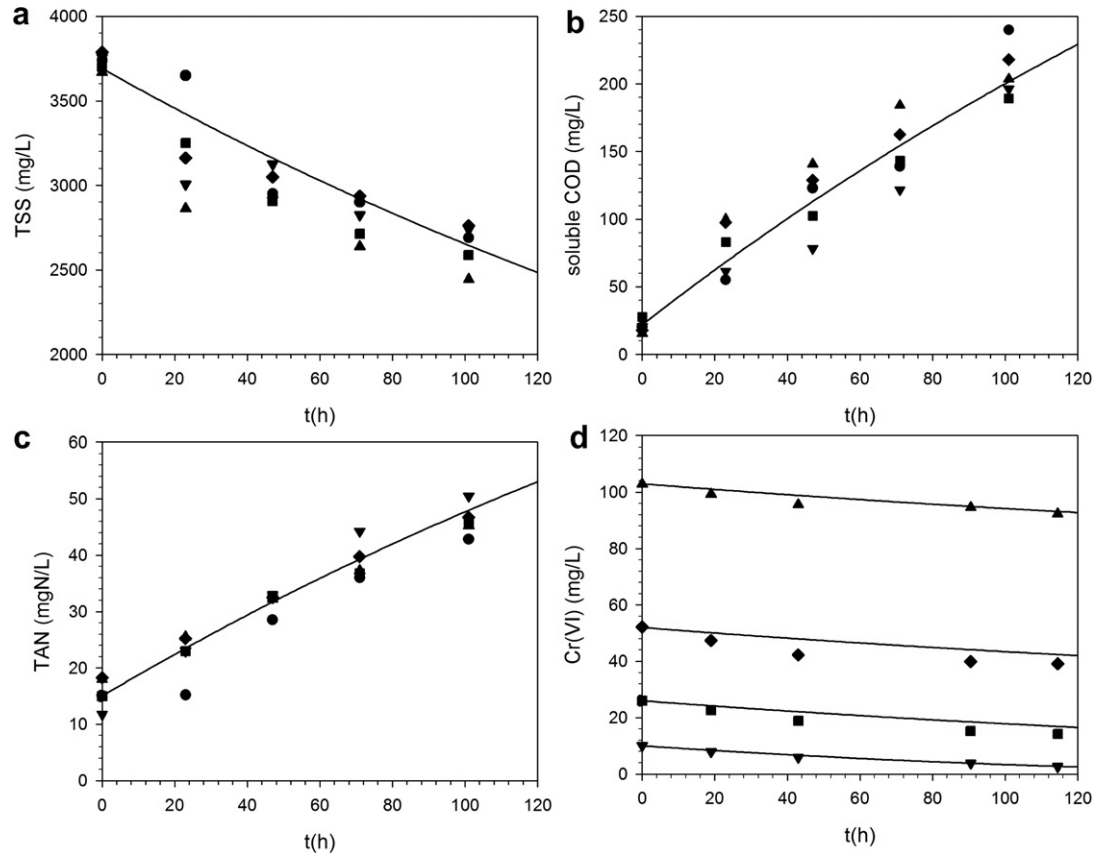


Fig. 1 – Time course of (a) total suspended solids (TSS), (b) soluble COD, (c) total ammonia nitrogen (TAN), and (d) hexavalent chromium (Cr(VI)) in batch cultures. Tested initial Cr(VI) concentrations were the following: (●) 0 mgCr L⁻¹, (▼) 10 mgCr L⁻¹, (■) 25 mgCr L⁻¹, (◆) 50 mgCr L⁻¹, and (▲) 100 mgCr L⁻¹. Lines indicate the proposed model.

Table 2 – Coefficients of the proposed model.

Coefficient	Units	Value	Reference/experiment
k_A (cheese whey)	h ⁻¹	0.012	Ferro Orozco et al., 2010b
k_A (lactose)	h ⁻¹	0.013 ± 0.002	Section 4.3
μ_{m0} (cheese whey)	h ⁻¹	0.303 ± 0.004	Section 4.2
μ_{m0} (lactose)	h ⁻¹	0.176 ± 0.055	Section 4.3
$\mu_{m\infty}$ (cheese whey)	h ⁻¹	0.023 ± 0.001	Section 4.2
$\mu_{m\infty}$ (lactose)	h ⁻¹	0.001 ± 0.005	Section 4.3
q_{sm0} (cheese whey)	mgCOD mgCOD ⁻¹ h ⁻¹	0.519 ± 0.006	Section 4.2
q_{sm0} (lactose)	mgCOD mgCOD ⁻¹ h ⁻¹	0.413 ± 0.127	Section 4.3
$q_{sm\infty}$ (cheese whey)	mgCOD mgCOD ⁻¹ h ⁻¹	0.086 ± 0.001	Section 4.2
$q_{sm\infty}$ (lactose)	mgCOD mgCOD ⁻¹ h ⁻¹	0.018 ± 0.012	Section 4.3
K	L mgCr ⁻¹	0.453 ± 0.014	Section 4.2
K_S	mgCOD L ⁻¹	188	Ferro Orozco et al., 2010b
K_{NH}	mgN L ⁻¹	10	Contreras et al., 2008
b	h ⁻¹	$(3.3 \pm 0.4) \times 10^{-3}$	Section 4.1
q_{CrGm}	mgCr mgCOD ⁻¹ h ⁻¹	1.5×10^{-4}	Ferro Orozco et al., 2008
q_{CrDm}	mgCr mgCOD ⁻¹ h ⁻¹	$(2.2 \pm 1.0) \times 10^{-5}$	Section 4.1
$i_{N,BM}$	mgN mgCOD ⁻¹	0.07	Gujer et al., 1999
$i_{N,P}$	mgN mgCOD ⁻¹	0.045 ± 0.005	Section 4.1
f_P	mgCOD mgCOD ⁻¹	0.133 ± 0.002	Section 4.1
R_C	mgCr mgCOD ⁻¹	0.019	Ferro Orozco et al., 2008
i_{SS}	mgSS mgCOD ⁻¹	0.77	Gujer et al., 1999

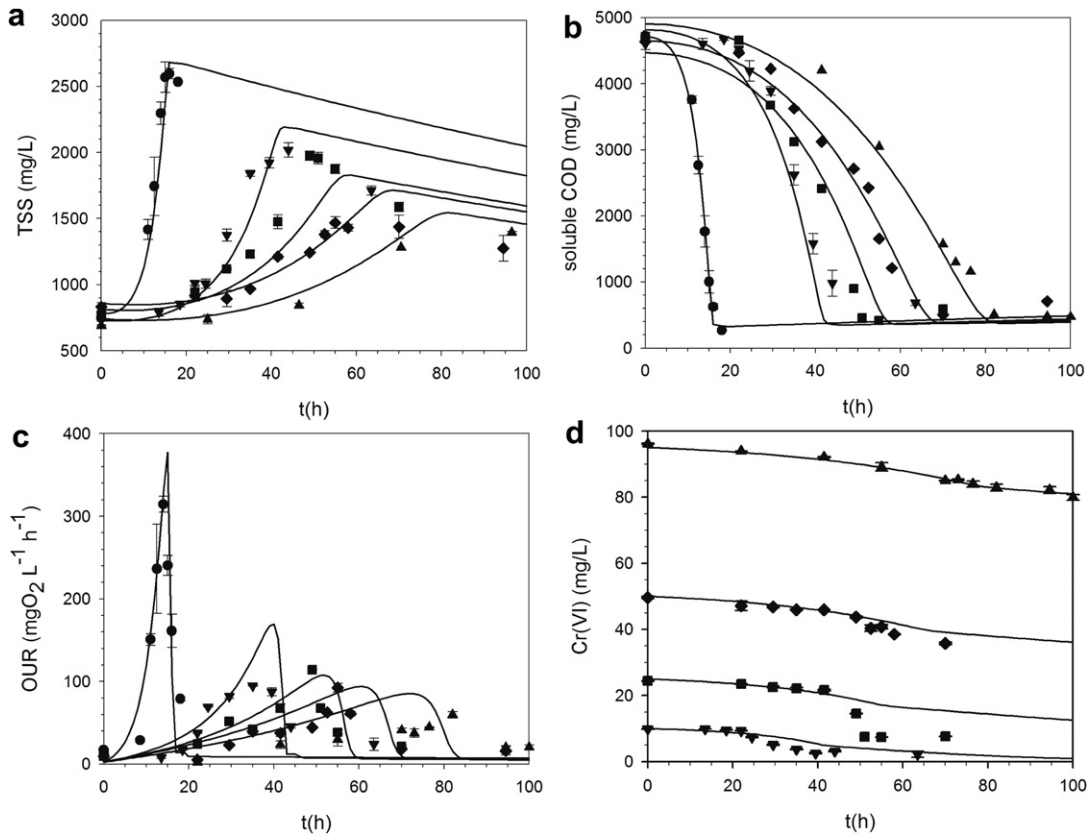


Fig. 2 – Time course of (a) total suspended solids (TSS), (b) soluble COD, (c) oxygen uptake rate (OUR), and (d) hexavalent chromium (Cr(VI)) in batch cultures with cheese whey as the carbon source. Cr(VI) initial concentrations were: (●) 0 mgCr L⁻¹, (▼) 10 mgCr L⁻¹, (■) 25 mgCr L⁻¹, (◆) 50 mgCr L⁻¹, and (▲) 100 mgCr L⁻¹. Lines indicate the proposed model.

those authors may provide good results regarding the effect of metals on the lag phase, a mathematically simpler approach such as the proposed in the present work was enough to represent our experimental results with an acceptable accuracy (Fig. 2).

The inhibition term in Eq. (2) is similar to the one proposed by other authors (Yamamoto et al., 1993; Elangovan and Philip, 2009). Fig. 3 shows the effect of Cr(VI) on the dimensionless specific growth rate (μ_m/μ_{m0}) calculated by Eq. (1) using the values for μ_{m0} , $\mu_{m\infty}$, and K shown in Table 2; for comparison purposes, literature data concerning the effect of Cr(VI) of the ratio μ_m/μ_{m0} are also depicted. In agreement to the proposed expression (Eq. 1), in all cases a similar trend can be observed. Hexavalent chromium exerts a strong inhibition on μ_m within the concentration range 0–20 mgCr L⁻¹; then, a much lesser effect of Cr(VI) on μ_m can be noticed for higher Cr(VI) concentrations (Fig. 3).

The proposed model also predicts that the true biomass yield (Y) decreases as a function of Cr(VI). This effect of Cr(VI) on Y is in accordance with results of Fig. 2a which shows that the maximum biomass concentration decreases as a function of the initial Cr(VI) concentration. In addition, several authors report this effect of Cr(VI) on Y (Srinath et al., 2002; Juvera-Espinosa et al., 2006; Villegas et al., 2008). According to Rittmann and Saez (1993), this behavior is typical of inhibitors

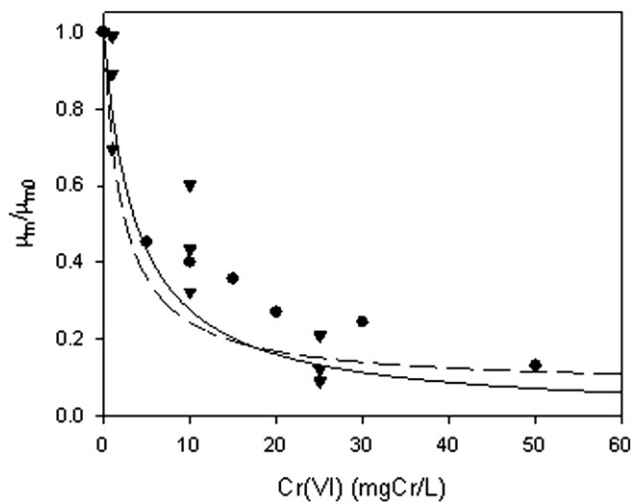


Fig. 3 – Effect of Cr(VI) on the dimensionless specific growth rate (μ_m/μ_{m0}) calculated with Eq. (1) using the coefficients shown in Table 2 (dotted line) and those adapted from Elangovan and Philip (2009) (continuous line), Bae et al. (2000) (circles), and Stasinakis et al. (2002) (triangles).

that uncouple substrate oxidation and biomass synthesis. Uncouplers usually make the cytoplasmatic membrane permeable for protons, lowering the proton motive force across the membrane and therefore, the amount of ATP synthesized per unit of substrate oxidized. Because ATP and biomass synthesis are related, as a result, the presence of uncouplers lowers the biomass yield. The effect of Cr(VI) on lowering the biomass yield can be explained taking into account that the reduction of chromate to Cr(III) is a proton-consuming reaction (Katz and Salem, 1994); thus, this reaction could lower the proton motive force across the cytoplasmatic membrane, in a similar manner than an uncoupler.

4.3. Effect of the initial nitrogen to carbon ratio (N_0/S_0) on activated sludge growth and Cr(VI) removal

Fig. 4 shows some examples of the time course of biomass (X), soluble COD, total ammonia nitrogen (TAN), and Cr(VI) for different initial TAN concentrations. In these cases, cheese whey was replaced by lactose as the carbon source in order to control the initial nitrogen to carbon ratio (N_0/S_0). In general, the lag phases observed in these experiments (Fig. 4) were longer than the corresponding to the experiment with cheese whey as the carbon source in the presence of 25 mgCr L⁻¹ (Fig. 2). While the lag phase with lactose was about 70 h, only 30 h was necessary to observe growth when cheese whey was tested. This difference in the lag phase occurred because the

model wastewater used to feed the parent activated sludge reactor had cheese whey as the carbon source, thus, microorganisms were adapted to this substrate but not to lactose. Fig. 2 shows that in the experiments with cheese whey, the increase in Cr(VI) concentration produced longer lag phases. Conversely, the lag phase observed in the experiments with lactose was constant (Fig. 4); taking into account that in these experiments the initial Cr(VI) concentration was constant, this result confirms that the lag phase depended on the Cr(VI) concentration but not on the ratio N_0/S_0 .

Fig. 4 shows that the removal of Cr(VI) in the absence of a nitrogen source was very low. When the initial TAN concentration was 250 mgN L⁻¹, the soluble COD (lactose) was almost depleted but TAN values were about 70 mgN L⁻¹ at $t = 140$ h; therefore, this case corresponded to a carbon-limited assay (high N_0/S_0 ratio). Beyond this time, Cr(VI) removal rate drastically decreased and TAN concentration increased due to the biomass decay. When the initial TAN concentration was 60 mgN L⁻¹, the nitrogen source was depleted at $t = 90$ h; although the carbonaceous substrate concentration was around 3000 mgCOD L⁻¹, the biomass growth stopped. Hence, in this case the biomass growth was limited by the nitrogen source (low N_0/S_0 ratio). Because lactose was the carbon but also the energy source, biomass concentration remained almost constant; however, Cr(VI) removal rate decreased due to the depletion of the nitrogen source.

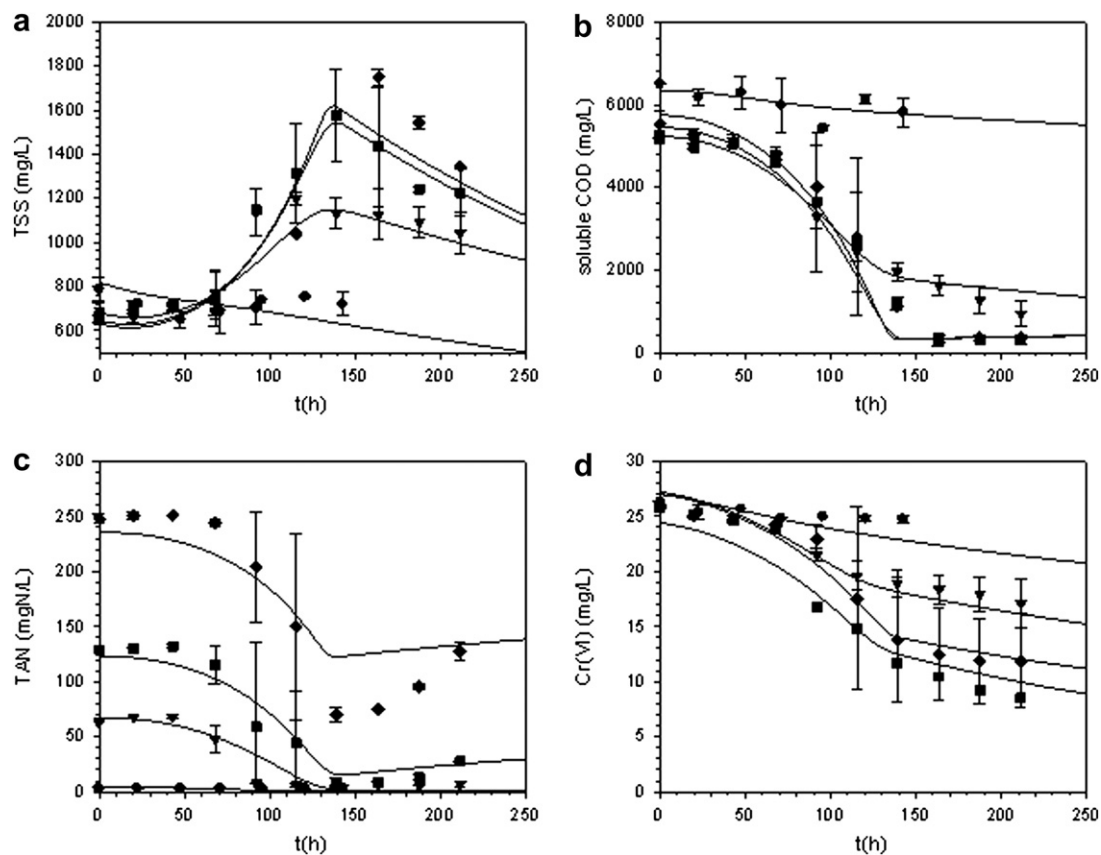


Fig. 4 – Time course of (a) total suspended solids (TSS), (b) soluble COD, (c) total ammonia nitrogen (TAN), and (d) hexavalent chromium (Cr(VI)) in batch cultures with lactose as the carbon source. Initial TAN concentrations were: (●) 0 mgN L⁻¹, (▼) 60 mgN L⁻¹, (■) 130 mgN L⁻¹, and (◆) 250 mgN L⁻¹. Lines indicate the proposed model.

The following coefficients of the proposed model were fitted to the Cr(VI) removal experiments with different initial TAN concentrations: K_A , μ_{m0} , $\mu_{m\infty}$, q_{Sm0} , $q_{Sm\infty}$; these coefficients were adjusted because they represent the growth kinetics of activated sludge using lactose as the carbon source. Table 2 shows that the kinetic coefficients corresponding to the growth of activated sludge using cheese whey were higher than those obtained with lactose. In contrast, K_A values corresponding to both substrates were similar. The true biomass growth yield (Y) values in the absence of Cr(VI) calculated by means of Eq. (5) for cheese whey and lactose were 0.58 and 0.43 gCOD gCOD⁻¹, respectively. These results indicate that the growth of activated sludge is favored by a complex carbon source, such as cheese whey, in comparison with a defined medium with lactose as the carbon source. Fig. 4 shows that the proposed model predicts quite well the values for biomass, soluble COD, TAN, and Cr(VI) as a function of time for all the tested conditions.

The effect of the ratio between initial concentration of the nitrogen source and the carbonaceous substrate (N_0/S_0) on the removal of Cr(VI) is shown in Fig. 5; in all cases, Cr(VI) removal was calculated at $t = 140$ h Cr(VI) removal increased from 2 mgCr L⁻¹ in the case of assays without nitrogen source addition ($N_0/S_0 = 0$ mgN gCOD⁻¹) to about 15 mgCr L⁻¹ for N_0/S_0 ranging between 19 and 28 mgN gCOD⁻¹. Further increments on the ratio N_0/S_0 did not enhance the removal of Cr(VI) because the carbonaceous substrate was completely consumed before the nitrogen source; in these cases, growth and Cr(VI) removal were limited by the carbonaceous source.

The initial N_0/S_0 ratio determines the substrate that limits the biomass growth. The stoichiometric N_0/S_0 ratio, $(N_0/S_0)_{St}$,

can be defined as the initial N_0/S_0 ratio at which both N and S are depleted at the same time; in this case both N and S are limiting substrates simultaneously. If N_0/S_0 is higher than $(N_0/S_0)_{St}$, N is in excess with respect to the stoichiometric requirements and S will be the growth limiting substrate. Conversely, when N_0/S_0 is lower than $(N_0/S_0)_{St}$, the carbonaceous substrate is in excess with respect to the stoichiometric requirements and N will limit the biomass growth. If assimilation (incorporation of the nitrogen source into biomass) is the only nitrogen consumption process (e.g. if nitrification can be neglected), $(N_0/S_0)_{St}$ can be calculated as the product between the nitrogen content of the biomass ($i_{N,BM}$), and the biomass growth yield (Y). Although the value corresponding to $i_{N,BM}$ for activated sludge can be considered as a constant, Y depends on many factors, such as wastewater characteristics, culture conditions, and the presence of toxic compounds (e.g. Cr(VI)). Using the values of the coefficients μ_{m0} , $\mu_{m\infty}$, q_{Sm0} , and $q_{Sm\infty}$ shown in Table 2 corresponding to lactose, Y was calculated as a function of Cr(VI) by combining Eqs. (1), (2), and (5); then, considering $i_{N,BM} = 0.07$ mgN mgCOD⁻¹, $(N_0/S_0)_{St}$ was calculated as a function of Cr(VI). Because Y varies with Cr(VI), calculated $(N_0/S_0)_{St}$ values also depended on Cr(VI); thus, two limiting conditions were considered. If the consumption of Cr(VI) is negligible then Cr(VI) = 25 mgCr L⁻¹ (the initial Cr(VI) concentration in these experiments); in this case $(N_0/S_0)_{St} = 21$ mgN gCOD⁻¹. Conversely, if Cr(VI) is depleted then $(N_0/S_0)_{St} = 30$ mgN gCOD⁻¹. Fig. 5 shows that this range was in accordance to the experimental values (19–28 mgN gCOD⁻¹).

4.4. Cr(VI) removal in continuous systems and model validation

The removal of Cr(VI) using activated sludge reactors operated at two sludge ages (20 and 45 d) and different inlet Cr(VI) concentrations were studied; in all cases cheese whey was the carbon source. Fig. 6a shows that steady-state values of TSS decreased as the inlet Cr(VI) concentration increased. This effect is in accordance with the decrease of the biomass as a function of the initial Cr(VI) concentration shown in Fig. 2a, confirming that the biomass yield (Y) decreases as a function of Cr(VI). Besides, no trend can be observed with respect to steady-state values of the soluble COD and TAN (Fig. 6b,c). In addition, Fig. 6d shows that the Cr(VI) in the outlet stream increased as a function of the inlet Cr(VI) concentration.

Steady-state values of TSS, soluble COD, TAN and Cr(VI) measured in continuous systems were compared to steady-state values calculated by the proposed model using the coefficients shown in Table 2 corresponding to cheese whey as the carbon source. Fig. 6 shows that, taking into account the experimental errors, in all cases model calculations were in agreement with the experimental results. Moreover, Fig. 7 shows that the model accurately predicts the transient concentrations of Cr(VI) as a function of time in response of step changes in the inlet Cr(VI) concentration. These results demonstrate that the proposed model could be a powerful tool to predict the effect of the operating conditions on the performance of an activated sludge reactor treating Cr(VI)-containing wastewaters in the presence of a readily biodegradable organic matter (cheese whey in this work) under fully aerobic conditions. The presence of high organic matter

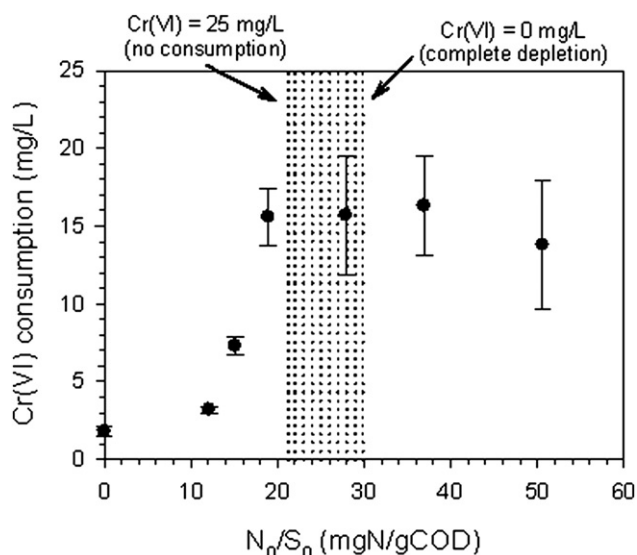


Fig. 5 – Effect of the initial nitrogen to carbon ratio (N_0/S_0) on the removal of Cr(VI). Initial conditions: Cr(VI) = 25 mg L⁻¹, $X = 700 \pm 50$ mgTSS L⁻¹, Lactose = 5 g L⁻¹. In all cases Cr(VI) removal were calculated at $t = 140$ h. Bars indicate the standard deviation. The shaded band indicates the range of stoichiometric N_0/S_0 values obtained by the proposed model.

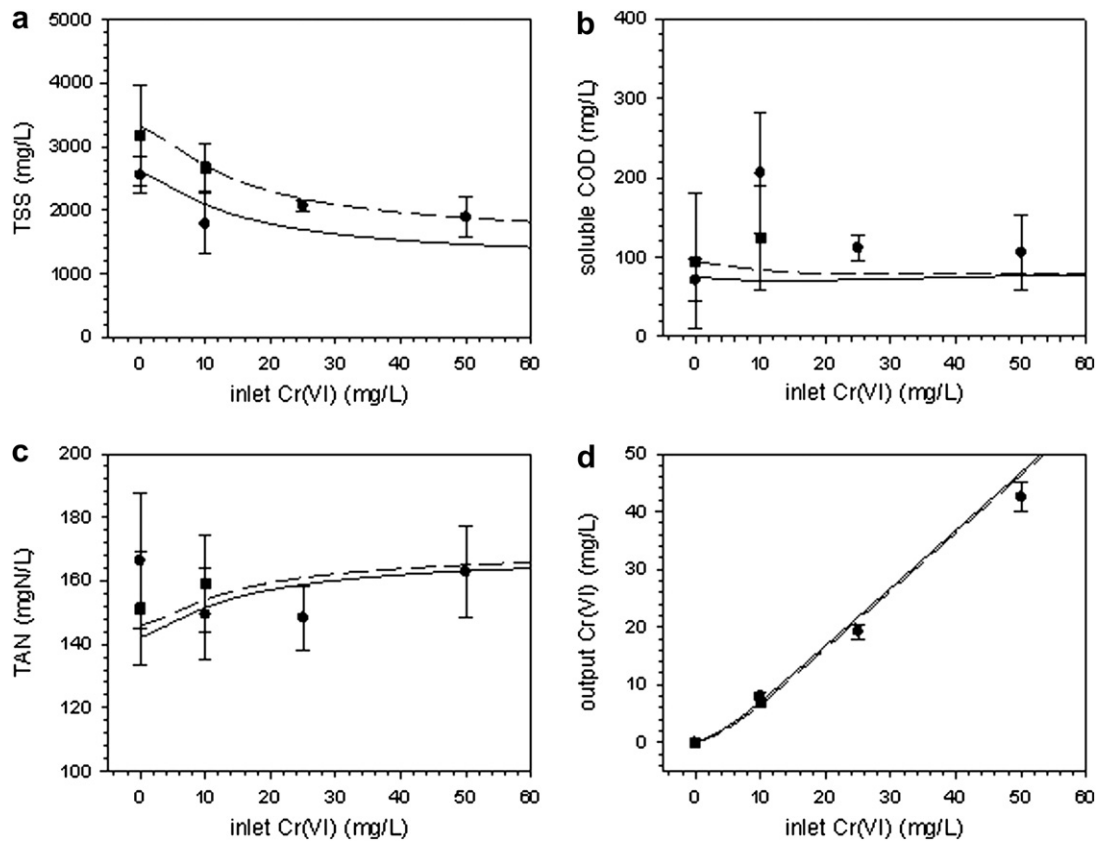


Fig. 6 – Steady-state values of (a) total suspended solids (TSS), (b) soluble COD, (c) total ammonia nitrogen (TAN), and (d) hexavalent chromium (Cr(VI)) as a function of the inlet Cr(VI) concentration in continuous systems feed with cheese whey as the carbon source and operating at different sludge ages: (●, continuous line) 20 d; (■, dashed line) 45 d. In all cases the hydraulic retention time was 2 d. Dots indicate experimental results, bars show the standard deviation. Lines indicate the proposed model.

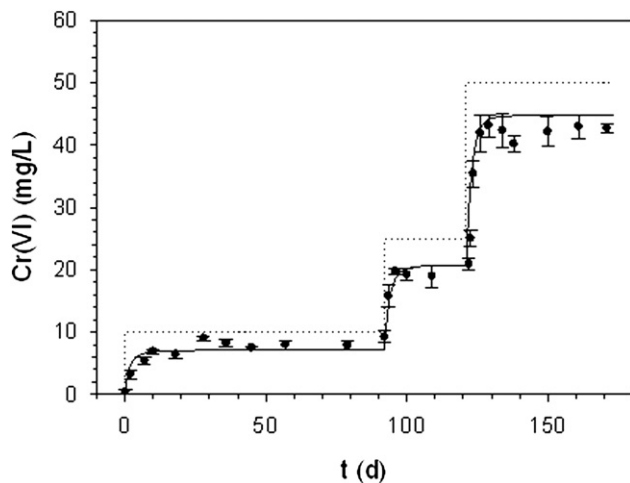


Fig. 7 – Time course of Cr(VI) in a continuous activated sludge reactor feed with cheese whey as the carbon source and operating at a sludge age of 20 d and hydraulic retention time of 2 d. Bars indicate the standard deviation. Dotted line indicates the inlet Cr(VI) concentration. Continuous line represents the proposed model.

concentrations along with Cr(VI) can occur when wastewaters from more than one industry are mixed (Elangovan and Philip, 2009; Cokgor et al., 2008, 2009). In the case of Cr(VI)-containing wastewaters with low organic matter content, such as electroplating, pigmentation, and wood preservation (Katz and Salem, 1994), a carbon source has to be supplied externally; thus, the addition of cheese whey (a residue from dairy industries) could be a suitable alternative to enhance the Cr(VI) reduction due to its low cost.

5. Conclusions

The mathematical model developed in the present work adequately describes the biological reduction of Cr(VI), carbon and nitrogen sources consumption, and biomass growth under fully aerobic conditions. Model coefficients were obtained by adjusting the model to the results obtained in batch cultures under different conditions such as: in the absence of carbon and nitrogen sources, different initial Cr(VI) concentrations, two carbon sources, and different initial nitrogen to carbon ratio. Then, the calibrated model was used to calculate steady-state values of TSS, soluble COD, TAN and

Cr(VI) in continuous systems, obtaining a good accordance with the experimental data. The model also accurately predicted the transient concentration of Cr(VI) in continuous systems as a function of time in response to step changes of the inlet Cr(VI) concentration. The proposed model could be a powerful tool to predict the effect of the operating conditions on the performance of an activated sludge reactor treating Cr(VI)-containing wastewaters in the presence of a readily biodegradable organic matter under fully aerobic conditions.

Acknowledgments

The authors gratefully acknowledge the financial support given by Universidad Nacional de La Plata (UNLP), Consejo Nacional de Investigaciones Científicas y Técnicas (CONICET), and Agencia Nacional de Promoción Científica y Tecnológica Argentina (ANPCyT).

Appendix. Supplementary data

Supplementary data related to this article can be found online at [doi:10.1016/j.watres.2011.03.011](https://doi.org/10.1016/j.watres.2011.03.011).

REFERENCES

- APHA, 2005. Standard methods for the examination of water and wastewater. In: Eaton, A.D., Clesceri, L.S., Rice, E.W., Greenberg, A.E., Franson, M.A.H. (Eds.), 21st ed. American Public Health Association, American Water Works Association, Water Environment Federation, USA (centennial edition).
- Bae, W.C., Kang, T.G., Kang, I.K., Won, Y.J., Jeong, B.C., 2000. Reduction of hexavalent chromium by *Escherichia coli* ATCC 33456 in batch and continuous cultures. *The Journal of Microbiology* 38 (8), 36–39.
- Cokgor, E.U., Insel, G., Aydin, E., Orhon, D., 2009. Respiriometric evaluation of a mixture of organic chemicals with different biodegradation kinetics. *Journal of Hazardous Materials* 161 (1), 35–41.
- Cokgor, E.U., Karahan, O., Orhon, D., 2008. The effect of mixing pharmaceutical and tannery wastewaters on the biodegradation characteristics of the effluents. *Journal of Hazardous Materials* 156 (1–3), 292–299.
- Contreras, E.M., Ferro Orozco, A.M., Zaritzky, N.E. Factors affecting the biological removal of hexavalent chromium using activated sludges. In: Balart M. (Ed.) *Management of Hazardous Residues Containing Cr(VI)*. Nova Science Publishers, Inc. New York, in press.
- Contreras, E.M., Ruiz, F., Bertola, N.C., 2008. Kinetic modelling of inhibition of ammonia oxidation by nitrite under low dissolved oxygen conditions. *Journal of Environmental Engineering* 134 (3), 184–190.
- Elangovan, R., Philip, L., 2009. Performance evaluation of various bioreactors for the removal of Cr(VI) and organic matter from industrial effluent. *Biochemical Engineering Journal* 44 (2–3), 174–186.
- Ferro Orozco, A.M., Contreras, E.M., Bertola, N.C., Zaritzky, N.E., 2007. Hexavalent chromium removal using aerobic activated sludge batch systems added with powdered activated carbon. *Water SA* 33 (2), 239–244.
- Ferro Orozco, A.M., Contreras, E.M., Zaritzky, N.E., 2008. Modelling Cr(VI) removal by a combined carbon-activated sludge system. *Journal of Hazardous Materials* 150 (1), 46–52.
- Ferro Orozco, A.M., Contreras, E.M., Zaritzky, N.E., 2010a. Cr(VI) reduction capacity of activated sludge as affected by nitrogen and carbon sources, microbial acclimation and cell multiplication. *Journal of Hazardous Materials* 176 (1–3), 657–665.
- Ferro Orozco, A.M., Contreras, E.M., Zaritzky, N.E., 2010b. Dynamic response of combined activated sludge-powdered activated carbon batch systems. *Chemical Engineering Journal* 157 (2–3), 331–338.
- Garbisu, C., Alkorta, I., Llama, M.J., Serra, J.L., 1998. Aerobic chromate reduction by *Bacillus subtilis*. *Biodegradation* 9 (2), 133–141.
- Gikas, P., Romanos, P., 2006. Effects of tri-valent (Cr(III)) and hexavalent (Cr(VI)) chromium on the growth of activated sludge. *Journal of Hazardous Materials* 133 (1–3), 212–217.
- Gikas, P., Sengor, S.S., Ginn, T., Moberly, J., Peyton, B., 2009. The effects of heavy metals and temperature on microbial growth and lag. *Global NEST Journal* 11 (3), 325–332.
- Guertin, J., Jacobs, J.A., Avakian, C.P., 2005. *Chromium (VI) Handbook*. IETEG: Independent Environmental Technical Evaluation Group. CRC Press.
- Gujer, W., Henze, M., Mino, T., van Loosdrecht, M., 1999. Activated sludge model no. 3. *Water Science and Technology* 39 (1), 183–193.
- Juvera-Espinosa, J., Morales-Barrera, L., Cristianí-Urbina, E., 2006. Isolation and characterization of a yeast strain capable of removing Cr(VI). *Enzyme and Microbial Technology* 40 (1), 114–121.
- Katz, S.A., Salem, H., 1994. *The Biological and Environmental Chemistry of Chromium*. VCH Publishers Inc., New York, USA.
- Li, Y., Low, G.K.-C., Scott, J.A., Amal, R., 2007. Microbial reduction of hexavalent chromium by landfill leachate. *Journal of Hazardous Materials* 142 (1–2), 153–159.
- McLean, J.S., Beveridge, T.J., 2001. Chromate reduction by a pseudomonad isolated from a site contaminated with chromated copper arsenate. *Applied and Environmental Microbiology* 67 (3), 1076–1084.
- McLean, J.S., Beveridge, T.J., Phipps, D., 2000. Isolation and characterization of chromium-reducing bacterium from a chromated copper arsenate-contaminated site. *Environmental Microbiology* 2 (6), 611–619.
- Megharaj, M., Avudainayagam, S., Naidu, R., 2003. Toxicity of hexavalent chromium and its reduction by bacteria isolated from soil contaminated with tannery waste. *Current Microbiology* 47, 51–54.
- Mendes, P., 1993. GEPASI: a software package for modelling the dynamics, steady states and control of biochemical and other systems. *Computer Applications in the Biosciences* 9 (5), 563–571.
- Mendes, P., Kell, D.B., 1998. Non-linear optimization of biochemical pathways: applications to metabolic engineering and parameter estimation. *Bioinformatics* 14 (10), 869–883.
- Michel, C., Brugna, M., Aubert, C., Bernadac, A., Bruschi, M., 2001. Enzymatic reduction of chromate: comparative studies using sulfate-reducing bacteria. Key role of polyheme cytochromes c and hydrogenases. *Applied Microbiology and Biotechnology* 55 (1), 95–100.
- Middleton, S.S., Latmani, R.B., Mackey, M.R., Ellisman, M.H., Tebo, B.M., Criddle, C.S., 2003. Cometabolism of Cr(VI) by *Shewanella oneidensis* MR-1 produces cell-associated reduced chromium and inhibits growth. *Biotechnology and Bioengineering* 83 (6), 627–636.
- Pattanapitpaisal, P., Brown, N.L., Macaskie, L.E., 2001. Chromate reduction and 16S rRNA identification of bacteria isolated

- from a Cr(VI)-contaminated site. *Applied Microbiology and Biotechnology* 57 (1–2), 257–261.
- Puzon, G.J., Petersen, J.N., Roberts, A.G., Kramer, D.M., Xun, L., 2002. A bacterial flavin reductase system reduces chromate to a soluble chromium(III)-NAD(+) complex. *Biochemical and Biophysical Research Communications* 294 (1), 76–81.
- Rittmann, B.E., Saez, P.B., 1993. Modeling biological processes involved in degradation of hazardous organic substrates. In: Levin, M., Gealt, M. (Eds.), *Biotreatment of Industrial and Hazardous Wastes*. McGraw Hill Book Co., New York, pp. 113–136.
- Sengor, S.S., Barua, S., Gikas, P., Ginn, T.R., Peyton, B., Sani, R.K., Spycher, N.F., 2009. Influence of heavy metals on microbial growth kinetics including lag time: mathematical modeling and experimental verification. *Environmental Toxicology and Chemistry* 28 (10), 2020–2029.
- Shen, H., Wang, Y.T., 1994. Biological reduction of chromium by *E. coli*. *Journal of Environmental Engineering* 120 (3), 560–572.
- Srinath, T., Verma, T., Ramteke, P.W., Garg, S.K., 2002. Chromium (VI) biosorption and bioaccumulation by chromate resistant bacteria. *Chemosphere* 48 (4), 427–435.
- Stasinakis, A.S., Mamais, D., Thomaidis, N.S., Lekkas, T.D., 2002. Effect of chromium (VI) on bacterial kinetics of heterotrophic biomass of activated sludge. *Water Research* 36 (13), 3341–3350.
- Stumm, W., Morgan, J.J., 1996. *Aquatic Chemistry. Chemical Equilibria and Rates in Natural Waters*, third ed. Wiley, New York. 425–513.
- US Environmental Protection Agency, 1998a. Toxicological review of hexavalent trivalent. In: Support of Summary Information on the Integrated Risk Information System (IRIS) (CAS No. 16065-83-1). US. Environmental Protection Agency, Washington, DC.
- US Environmental Protection Agency, 1998b. Toxicological review of hexavalent chromium. In: Support of Summary Information on the Integrated Risk Information System (IRIS) (CAS No.18540-29-9). US. Environmental Protection Agency, Washington, DC.
- Villegas, L.B., Fernández, P.M., Amoroso, M.J., de Figueroa, L.I.C., 2008. Chromate removal by yeast isolated from sediments of a tanning and a mine site in Argentina. *Biometals* 21 (5), 591–600.
- Wang, Y.T., Shen, H., 1995. Bacterial reduction of hexavalent chromium. *Journal of Industrial Microbiology and Biotechnology* 14 (2), 159–163.
- Wang, Y.T., Shen, H., 1997. Modeling Cr(VI) reduction by pure bacterial cultures. *Water Research* 31 (4), 727–732.
- Yamamoto, K., Kato, J., Yano, T., Ohtake, H., 1993. Kinetics and modeling of hexavalent chromium reduction in *Enterobacter cloacae*. *Biotechnology and Bioengineering* 41 (1), 129–133.